B1608

Composite conductivity of MIEC-based SOFC anodes: Implications for microstructure optimization

***Philip Marmet (1), Thomas Hocker (1), G. K. Boiger (1), Jan G. Grolig (2), Holger Bausinger (2), Andreas Mai (2), Mathias Fingerle (3), Sarah Reeb (3), Joseph M. Brader (4) and Lorenz Holzer (1)**

(1) Zurich University of Applied Sciences, Institute of Computational Physics 8401 Winterthur/Switzerland

(2) Hexis AG, 8404 Winterthur/Switzerland

(3) Math2Market GmbH, D-67657 Kaiserslautern/Germany

(4) University of Fribourg, Department of Physics, 1700 Fribourg/Switzerland

* Corresponding author: mame@zhaw.ch

Abstract

Fully ceramic anodes such as LSTN-CGO offer some specific advantages compared to conventional cermet anodes. Ceria- and titanate-based phases are both mixed ionic and electronic conductors (MIEC), which leads to very different reaction mechanisms and associated requirements for the microstructure design compared to e.g. Ni-YSZ. Due to the MIEC-property of both solid phases, the transports of neither the electrons nor the oxygen ions are limited to a single phase. As a consequence, composite MIEC electrodes reveal a remarkable property that can be described as 'composite conductivity' (for electrons as well as for ions), which is much higher than the (hypothetical) single phase conductivities of the same microstructure. In composite MIEC anodes, the charge carriers can reach the reaction sites even when the volume fraction of one MIEC phase is below the percolation threshold, because the missing contiguity is automatically bridged by the second MIEC phase. The MIEC properties thus open a much larger design space for microstructure optimization of composite electrodes.

In this contribution, the composite conductivities of MIEC-based anodes are systematically investigated based on virtual materials testing and stochastic modeling. For this purpose, a large number of 3D microstructures, representing systematic compositional variations of composite anodes, is created by microstructure modeling. The underlying stochastic model is fitted to experimental data from FIB-SEM tomography. For the fitting of the stochastic model, digital twins of the tomography data are created using the methodology of gaussian random fields. By interpolation between and beyond the digital twin compositions, the stochastic model then allows to create numerous virtual 3D microstructures with different compositions, but with realistic properties. The effect of microstructure variation on the composite conductivity is then determined with transport simulations for each 3D microstructure. Furthermore, the corresponding microstructure effects on the cell-performance are determined with a Multiphysics model that describes the anode reaction mechanism. Especially the impact of the composite conductivities on the cell performance is studied in detail. Finally, microstructure design regions are discussed and compared for three different anode materials systems: titanate-CGO (with composite conductivities), Ni-YSZ (with single-phase conductivities), Ni-CGO (with single-phase ionic and composite electronic conductivities).

1. Introduction

Solid oxide fuel cell (SOFC) technology is a promising solution for the efficient use of renewable fuels or natural gas for decentral heat and power generation. Ni-YSZ represents the anode composition that is most commonly used in SOFCs. Unfortunately, this material shows various types of degradation including Ni coarsening, carbon coking, sulfur poisoning and mechanical damage caused by redox cycling [1]. Moreover, the electrochemical reaction is bound to the triple phase boundaries, which induces a specific microstructure limitation towards the electrochemical activity in Ni-YSZ cermet anodes.
As an alternative anode concept, mixed ionic and electronic conductive (MIEC) materials are drawing much attention. An obvious advantage of MIEC materials is the fact that the fuel oxidation reaction can take place on the complete MIEC/pore interface. An already well-established MIEC material system is Ni-CGO. However, some of the issues associated with the Ni-degradation persist. Therefore, titanate-CGO anodes are considered [2], where the Ni-phase is replaced by a titanate-MIEC with a relatively high electronic conductivity. The fact that both phases are MIECs leads to very different reaction mechanisms and associated requirements for the microstructure design compared to e.g. Ni-YSZ as illustrated in Fig. 1. An obvious difference, which is widely discussed in literature, is the fact that in MIEC anodes the reaction is not restricted to the TPB's like in Ni-YSZ but takes place mainly on the CGO-pore interface. Another important difference, which is less prominently discussed in literature, considers the charge transport. In MIEC anodes the composite conductivities resulting from the conductivity contributions of both phases need to be considered, and not only the single-phase conductivities like for Ni-YSZ. Understanding the effect of composite conductivity on the anode performance is the main focus of this contribution. For completion it must be noted that the microstructure effects for the gas-transport in the pore-phase are equal for both material systems.

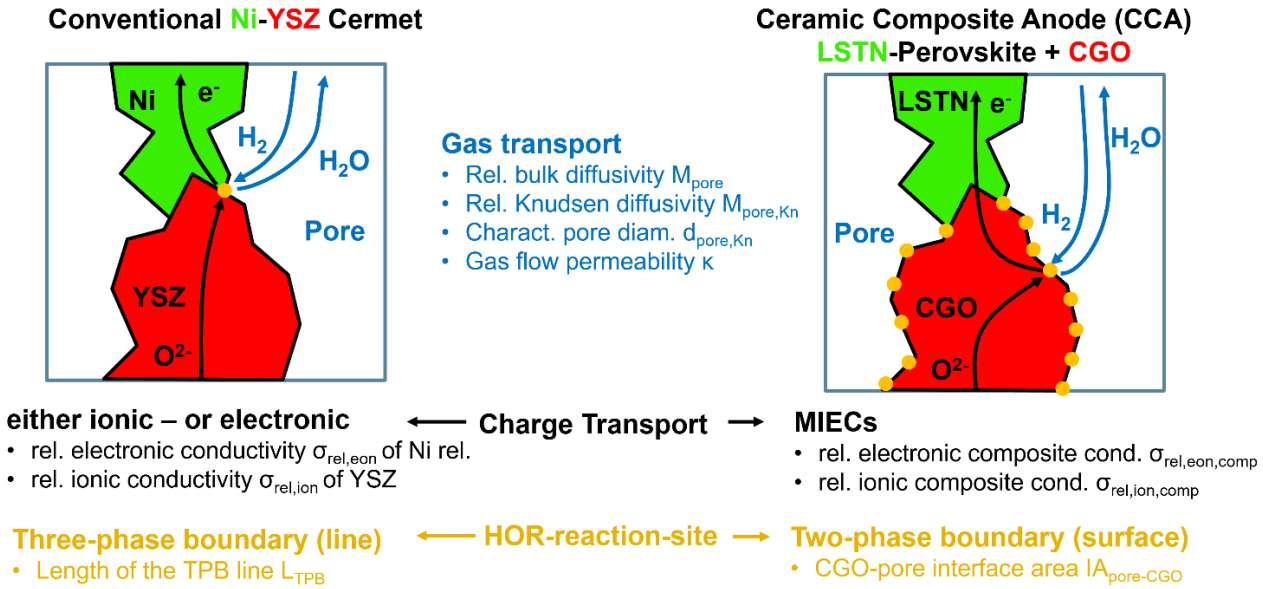

Figure 1: Comparison of the conduction pathways and (simplified) reaction mechanisms of a conventional Ni-YSZ anode and the novel titanate-CGO anode. For both systems, the microstructure parameters needed for physical modelling are stated for gas-transport, charge transport and reaction kinetics.

In this contribution, the microstructure design for the titanate-CGO system will be systematically studied using stochastic microstructure modeling and virtual materials testing. The findings will be compared to the Ni-YSZ and Ni-CGO material systems.

2. Digital Materials Design (DMD) for titanate-CGO anodes

In order to exploit the large design space opening due to the combination of two MIEC-phases, digital materials design (DMD) methodologies are used for an efficient and knowledge-based microstructure optimization.

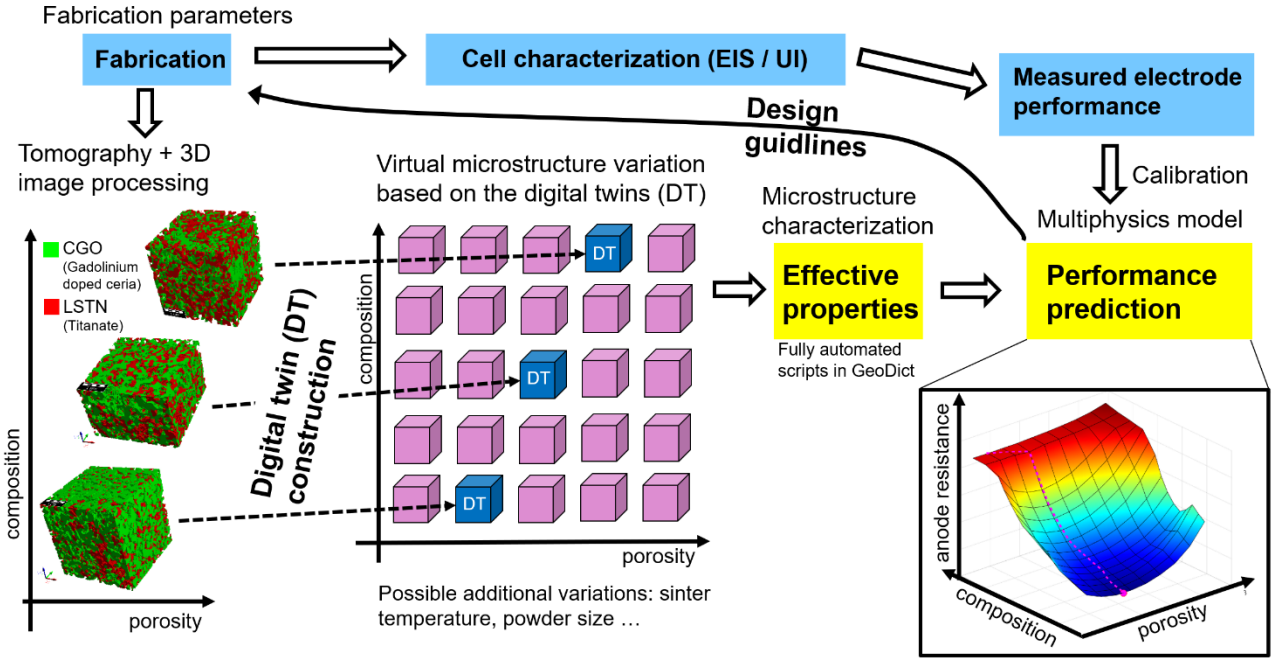

Figure 2: Overview of methodologies for Digital Microstructure Design (DMD).

With the digital microstructure design (DMD) approach, the effect of microstructure variation on the cell performance can be assessed. An overview of the DMD approach is provided in Fig. 2, including construction of stochastic digital twins for real microstructures, virtual variation of microstructures and prediction of the corresponding cell performances with a Multiphysics electrode model calibrated with experimental data.
The basis for the DMD-process is a set of fabricated SOFC-cells. The performances of the cells are experimentally characterized using electrochemical impedance spectroscopy (EIS). The real microstructures are captured using FIB-SEM tomography for a small number of fabricated cells with different compositions and porosities. Stochastic digital twins (i.e. microstructure descriptions based on stochastic geometry) with matching microstructure properties are then constructed for each real structure (i.e. for each data set from FIB-SEM tomography). The virtual structures are constructed with an approach that is based on pluri-gaussian random fields [3,4]. The phase volume fractions, specific interface areas, three-phase boundary lengths and effective transport properties of the virtual structures are matched to real structures from FIB-SEM tomography in order to obtain the digital twins. On that basis, the microstructure can be varied for a large parameter space in a realistic way. In the current study, the compositions (i.e. relative phase volume fractions) are varied in the range of LSTN:CGO = 90:10 to 10:90. In addition, also the total solid volume fractions (which are equivalent to 100% – porosity) are varied from 40% to 80%. Microstructure analysis enables to quantify all relevant morphological characteristics (tortuosity, constrictivity, TPB as well as surface and interface areas). Furthermore, virtual testing by 3D numerical simulation is used to characterize the associated effective or relative transport properties.
In Fig. 3 a) the specific CGO-pore interface area and in Fig. 3 b) the three-phase boundary length are reported as a function of total solid volume fraction (ϕ_{tot} = 100 % – porosity) and

composition ($\phi_{CGO,\ rel}$ = relative volume fraction of CGO). Both parameters represent potential reaction sites and are thus important for the reaction kinetics. However, they show their maxima at different locations. In Fig. 3 c), the relative ionic composite conductivities and in Fig. 3 d) the relative electronic composite conductivities are reported as a function of the total volume fraction and composition. The definition of the relative composite conductivities will be introduced in section 3.2. The relative ionic composite conductivity is maximal for a large total solid volume fraction (i.e. low porosity) and a high CGO content, because of the relatively high intrinsic ionic conductivity of CGO. The relative electronic composite conductivity is maximal for a large total solid volume fraction and a high LSTN content (i.e. low CGO content), because of the relatively high intrinsic electronic conductivity of LSTN.

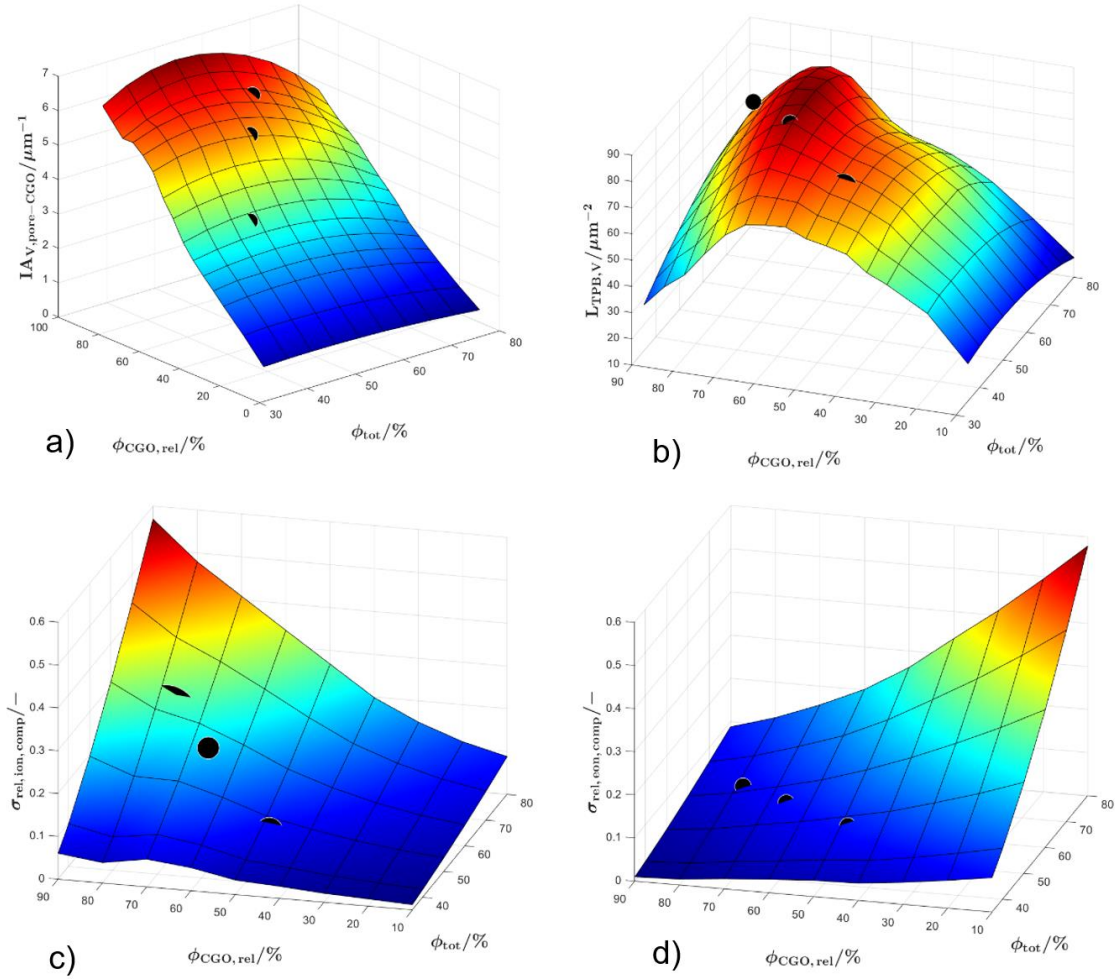

Figure 3: Specific CGO-pore interface area a), specific three-phase boundary length b), relative ionic composite conductivity c) and relative electronic composite conductivity d) as a function of the total volume fraction (ϕ_{tot}) and the relative volume fraction of CGO ($\phi_{CGO,\ rel}$). Black dots mark the properties of experimental data from FIB-SEM tomography.

A Multi-physics simulation model is then used to predict the impact of the microstructure variation on the electrode performance (i.e. area specific resistance ASR_{tot}). For the simulation we adapted a 1D FE-model for ceria-based anodes from Marmet et al. [5]. The reaction kinetics are calibrated to the experimental data of Burnat et al. [2], where a similar material system (i.e. titanate-CGO) was investigated. The fitting of the experimental data suggests that the main electrochemical activity is related to a reaction on the CGO-pore interface and that there is a considerably smaller contribution from the reaction at three-phase boundaries. The gas transport is modelled with the dusty gas model. The charge

transport is modelled by Ohms law, using an ionic and electronic potential. The microstructure effect is captured using the relative ionic and electronic composite conductivities reported in Fig. 3 c) and d). This approach of modelling the charge transport represents a considerable simplification of the transport mechanism in MIECs, which are governed by drift and diffusion. In [5], the charge transport in CGO has e.g. been modelled using the Nernst Planck Poisson equation. However, it is currently not clear how the drift and diffusion transport evolves across the CGO-titanite boundaries and a considerable amount of basic research is still needed for this material system. Therefore, we stick to this simplified but consistent description of charge transport by Ohms law.

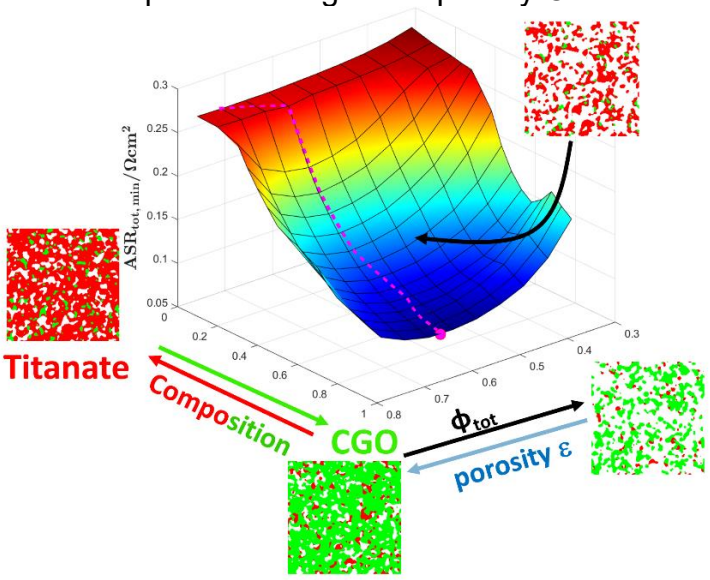

Figure 4: Total ASR (for the optimal anode-thickness) as a function of the total volume fraction (ϕ_{tot}) and the relative volume fraction of CGO (composition, i.e. $\phi_{CGO,\,rel}$).

As a result of this Multiphysics model, the total area specific resistance (ASR) of the anode model is reported in Fig. 4 as a function of the total solid volume fraction (ϕ_{tot}) and the composition ($\phi_{CGO,\,rel}$). Note that the ASR is calculated for varying anode-thicknesses and the ASR for the optimal anode-thickness is reported here. Hence, for each point on the composition grid, the optimal anode thickness is determined by a series of simulation runs and the corresponding minimal ASR is reported. The dashed magenta line represents the minimal ASR upon compositional variation. The optimal total volume fraction is thereby always around 65%, which is the result of a tradeoff between three competing microstructure effects: active CGO-pore interface area, relative gas diffusivity and relative composite conductivity for both, ionic and electronic charge transports. The systematic analysis reveals that the optimal anode composition is LSTN:CGO = 10:90 (relative solid volume fractions). This optimum represents the highest CGO-content that was investigated within the study. This result can be attributed to the fact that a larger CGO content provides a higher ionic conductivity and also a higher electrochemical activity due to the larger CGO-pore interface area. Hence, for titanate-rich anodes, a steep reduction of the ASR is observed when increasing the CGO contents. However, the curve for ASR changes is significantly flattening for anodes with high CGO contents. Moreover, in our 1D model we assume an ideal current collector on top of the active anode. It must be emphasized that a certain titanate content in the anode can also contribute to the current collector functionality. However, this contribution from the titanite phase cannot be captured with our 1D model. Therefore, the optimal composition in reality may deviate from the optimum model composition, since it also depends on broader aspects of the cell concept (including current collector and MIC architecture) and on the degradation behavior of the cell.

3. Composite conductivity

3.1 From single-phase to composite conductivity

In the common Ni-YSZ electrodes, ions and electrons are transported in separate phases as illustrated in Fig. 5 a). The effective single-phase conductivities respecting the microstructure influence can be expressed as:

$$\sigma_{\mathrm{eff,ion}} = \sigma_{\mathrm{rel,YSZ}} \cdot \sigma_{\mathrm{0,ion,YSZ}} \quad (1)$$

$$\sigma_{\mathrm{eff,eon}} = \sigma_{\mathrm{rel,Ni}} \cdot \sigma_{\mathrm{0,eon,Ni}} \quad (2)$$

The relative conductivities $\sigma_{\mathrm{rel,YSZ}}$ and $\sigma_{\mathrm{rel,Ni}}$ account for the microstructure limitations on conductive/diffusive transport and can be described quantitatively with phase volume fraction ϕ, tortuosity τ and constrictivity β of the transporting phase as described in [7]:

$$\sigma_{\mathrm{rel}}^{\mathrm{pred}} = \frac{\phi^{1.15}\beta^{0.37}}{\tau^{4.39}} \quad (3)$$

For the single-phase conductivities, the impact of intrinsic properties and microstructures can be described separately from each other. The relative conductivity is therefore also called microstructure factor (M-factor) since it describes purely geometric effects.

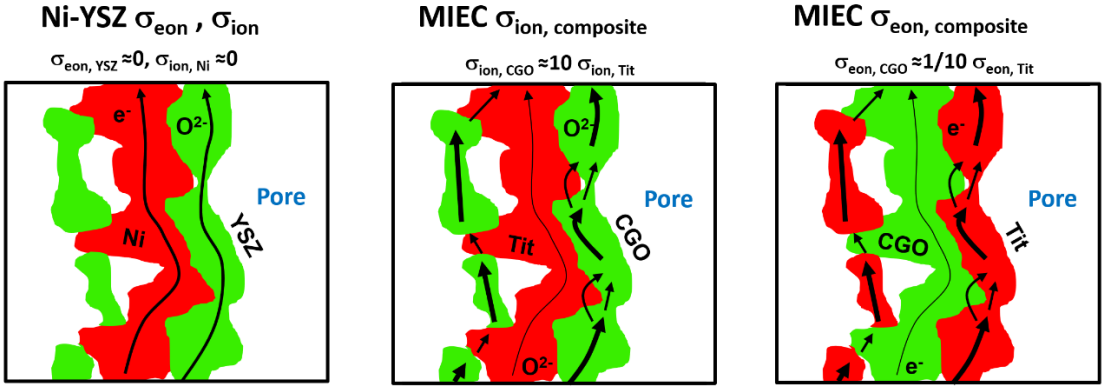

Figure 5: Illustration of the charge carrier pathways assuming different material properties for the same microstructure: a) Conventional Ni-YSZ anode with isolated conduction of electrons in the Ni-phase and ions in YSZ-phase, resulting in a hard restriction of percolation threshold, (i.e. no transport via isolated islands). b) In a titanate-CGO anode, the ions are predominantly transported in the CGO-phase due to the higher ionic conductivity. However, despite its relatively low ionic conductivity, the titanate phase is able to bridge islands, bottlenecks and tortuous pathways of the CGO-phase, which significantly enhances the ionic composite conductivity. c) Electrons in a titanate-CGO anode are predominantly transported in the titanate-phase due to its higher electronic conductivity. However, the electronic composite conductivity is significantly enhanced by the CGO-phase, despite its lower electronic conductivity, like vice versa for ions in b).

For the Ni-YSZ material system (Fig. 5 a)), the transport of electrons is restricted to the Ni-phase and the ion transport to the YSZ-phase. This means that disconnected components do not contribute to the reaction and bottlenecks have a strong effect on the relative conductivity. In contrast, for the titanate-CGO system (Fig. 5 b) and c)) the transports of neither the electrons nor the oxygen ions are limited to a single phase due to the MIEC-property of both solid phases. Hence, the transport limitations due to the microstructure of the single phases are less restrictive. Disconnected components (islands), bottlenecks and tortuous pathways can be bridged by the adjacent solid phase.

3.2 Definition of the ionic and electronic composite conductivities

In contrast to the effective single-phase conductivity, the effects of intrinsic properties and of the microstructure on the effective composite conductivity cannot be strictly separated. This is because the transport pathways extend over both solid phases and are a result of combined effects of the intrinsic conductivities and microstructure effects of both phases. In order to be able to provide a measure similar to the relative conductivity (or M-factor) for single solid phase systems, a relative ionic composite conductivity $\sigma_{\mathrm{rel,ion,comp}}$ and a relative electronic composite conductivity $\sigma_{\mathrm{rel,eon,comp}}$ is defined as follows.

$$\sigma_{\mathrm{eff,ion,comp}} = \sigma_{\mathrm{rel,ion,comp}} \sigma_{0,\mathrm{ion,SP1}} \quad (4)$$

$$\sigma_{\mathrm{eff,eon,comp}} = \sigma_{\mathrm{rel,eon,comp}} \sigma_{0,\mathrm{eon,SP2}} \quad (5)$$

where $\sigma_{\mathrm{eff,ion,comp}}$ and $\sigma_{\mathrm{eff,eon,comp}}$ are the effective ionic and electronic composite conductivities and $\sigma_{0,\mathrm{ion,SP1}}$ is the intrinsic ionic conductivity of the solid phase 1 (SP1) with the better ionic conductivity (i.e. CGO) and $\sigma_{0,\mathrm{eon,SP2}}$ is the intrinsic electronic conductivity of the solid phase 2 (SP2) with the better electronic conductivity (i.e. titanate). Therewith, the relative composite conductivity is a normalization of the effective composite conductivity with the intrinsic conductivity of the solid phase with the higher conductivity. As a consequence, the defined relative composite conductivities can be defined as functions of the ratio of the intrinsic conductivities of the two MIEC phases:

$$\sigma_{\mathrm{rel,ion,comp}} = \frac{\sigma_{\mathrm{eff,ion,comp}}}{\sigma_{0,\mathrm{ion,SP1}}} = f\left(\frac{\sigma_{0,\mathrm{ion,SP2}}}{\sigma_{0,\mathrm{ion,SP1}}}\right) \quad (6)$$

$$\sigma_{\mathrm{rel,eon,comp}} = \frac{\sigma_{\mathrm{eff,eon,comp}}}{\sigma_{0,\mathrm{eon,SP2}}} = f\left(\frac{\sigma_{0,\mathrm{eon,SP1}}}{\sigma_{0,\mathrm{eon,SP2}}}\right) \quad (7)$$

In this sense the relative composite conductivity can be interpreted as the microstructure effect for a specific ratio of the intrinsic conductivities. Hence, in contrast to the single-phase conductivity, for MIEC composites the impact of microstructure cannot be described fully independently from the intrinsic phase conductivities, but for a certain ratio thereof.

3.3 Effect of the composite conductivity

The composite conductivity shall be illustrated using a subset of the data presented in section 2 reported in Fig. 6 by fixing the composition to LSTN:CGO = 70:30 (i.e. constant relative phase volume fractions), while still varying the total solid volume fraction (or porosity, respectively). Despite the fact, that both phases can transport electrons and ions, the conductivities of the titanate and CGO are very different. For currently available titanates [6], the intrinsic electronic conductivity (ca. 10 S/cm) is about one order of magnitude higher than the intrinsic electronic conductivity of CGO (ca. 1 S/cm) for an operating temperature of 850°C. The intrinsic ionic conductivity of titanate (ca. 0.01 S/cm) is about one order of magnitude lower than the intrinsic ionic conductivity of CGO (ca. 0.1 S/cm). Nevertheless, the limiting effects from microstructure are much weaker in composite MIEC anodes compared to anodes with single phase conductivity (e.g. cermets), which leads to effective composite conductivities (for electrons as well as for ions), which are much higher than the (hypothetical) single phase conductivities of the same microstructure, as reported in Fig. 6. We select a fixed value for the total solid phase volume fraction ϕ_{tot} = 70% in Fig. 6 b) to illustrate different contributions to the relative ionic composite conductivity. The contribution from the relative single-phase ionic conductivity of CGO (green) is very low

($\sigma_{\mathrm{rel,CGO}} = 0.010$). In contrast, the relative single-phase conductivity of the titanate phase would be considerably higher ($\sigma_{\mathrm{rel,LSTN}} = 0.268$). However, because the intrinsic ionic conductivity of the titanate is one order of magnitude lower than the one of CGO, the true contribution of the isolated titanate phase is 10 times smaller (i.e. 0.027). Hence, we still have a missing part of 0.077 to the total ionic composite conductivity $\sigma_{\mathrm{rel,ion,comp}} = 0.115$. This difference between the ionic composite conductivity and the sum of the single-phase ionic conductivities can be interpreted as the composite conductivity effect. Compared to the hypothetical single-phase conductivity of CGO the ionic composite conductivity is 12 times higher (see Fig. 6 b, blue vs green lines)!

The composite conductivity effects due to MIEC properties are qualitatively illustrated in Fig. 5 b). CGO-particles that would otherwise (i.e. in materials with single phase conductivity) be disconnected from the main CGO-phase network, are now connected over the titanate-phase (resulting in higher effective volume fraction). Furthermore, the bottlenecks in the CGO-phase are less restrictive for ion transport because they can be bridged by the titanate phase (resulting in higher constrictivity). Finally, the ionic charge-carriers do not need to detour the obstacles represented by the titanite phase. Therefore, the bridging effects in MIEC composites also results in shorter pathways (i.e. lower tortuosity). Hence, the three main limiting effects from microstructure (see Eq. 3) are decreased in MIEC materials with composite conductivity.

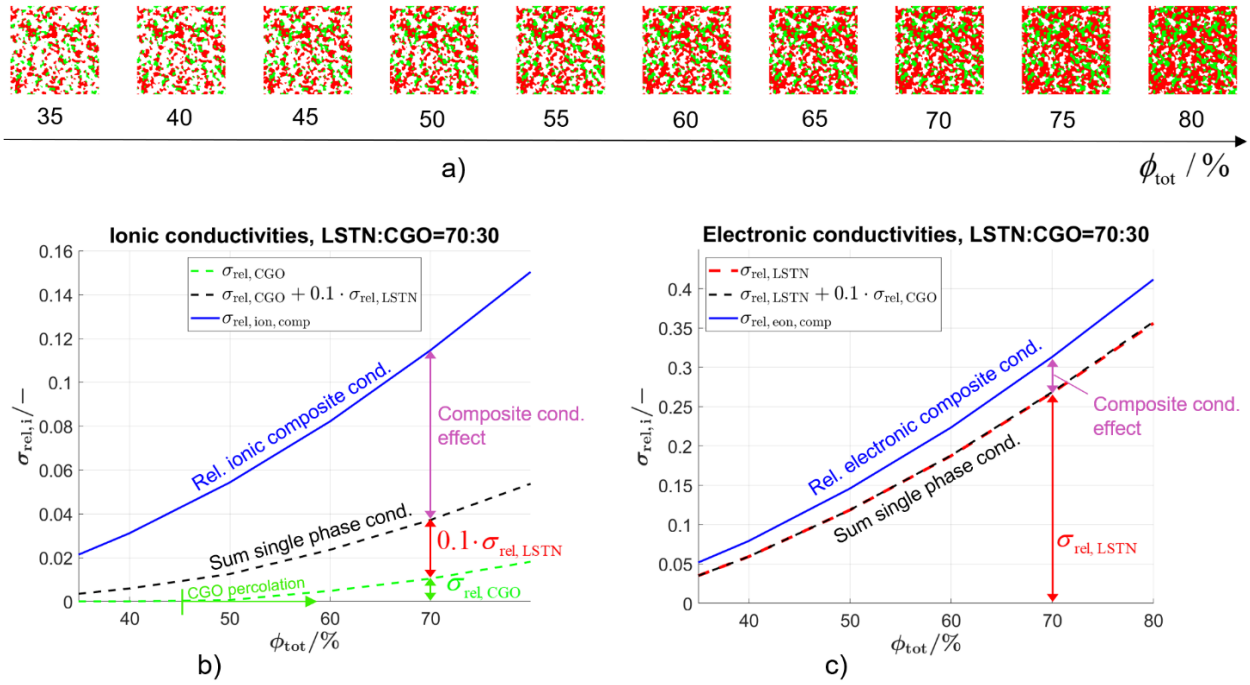

Figure 6: a) Virtual structures of ceramic composite anodes with 70% LSTN and 30% CGO for different total volume fractions (ϕ_{tot}), and b) illustration of the three contributions, which constitute the total ionic composite conductivity in MIEC anodes. These are the effective ionic conductivities of isolated LSTN and isolated CGO phases. In addition, there is a specific composite part, which originates from the fact that obstacles to ionic transport (e.g. bottlenecks and dead-ends) in one phase can be by-passed by ionic transport through the other phase. Note that the contribution from LSTN must be weighted by 0.1, because its intrinsic ionic conductivity is 10 times smaller compared to CGO. c) Vice versa for the electronic composite conductivity: In this case, the isolated CGO-part does not contribute significantly to the total composite conduction due to a combined effect from low intrinsic el. conductivity and low volume fraction. Nevertheless, there is still a considerable composite conductivity effect associated with CGO, which supports the overall electronic transport.

This composite conductivity effect is particularly important for the phase with the lower volume fraction. The charge carriers can reach the reaction sites even when the phase volume fraction(s) is/are below the percolation threshold. As shown in Fig. 6b), the CGO phase only percolates for ϕ_{tot} > 45%, but already for total volume fractions below this percolation threshold it contributes significantly to the total conductivity due to the bridging effect. For the electronic composite conductivity reported in Fig. 6 c) the isolated CGO-part does not contribute significantly because of its lower volume fraction and lower intrinsic conductivity. Nevertheless, there is a considerable composite conductivity effect from the CGO-phase, which supports the electronic charge transport in the titanate-phase.

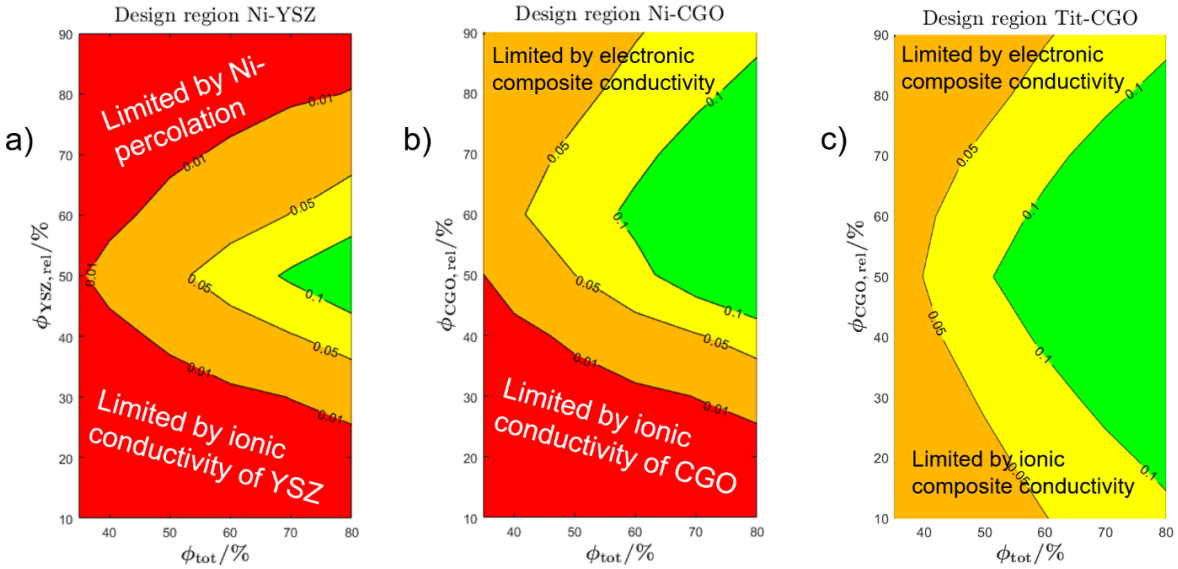

Figure 7: Illustration of the design regions for a) Ni-YSZ, b) Ni-CGO and c) titanate-CGO anodes. The red regions represent unsuitable design region with insufficient conductivity, while the green regions are ideal from a conductivity point of view.

In Fig. 7, the design regions from a conductivity point of view are compared for Ni-YSZ, Ni-CGO and titanate-CGO anodes in a simplified way. The red regions own insufficient conductivity and need to be avoided, while the green regions own good ionic and electronic conductivities. For all the three material systems, the same microstructure variations (as previously simulated for LSTN-CGO) are used. The contours of the design regions are defined as the smaller and therefore limiting value of the relative electronic or ionic conductivity. Specifically, the following expressions are used for the different materials:

- Ni-YSZ-like system: $\min\left(\sigma_{\mathrm{rel,Ni}}, \sigma_{\mathrm{rel,YSZ}}\right)$, where $\sigma_{\mathrm{rel,Ni}}$ and $\sigma_{\mathrm{rel,YSZ}}$ are the single-phase relative conductivities of the Ni-phase and YSZ-phase. Ni = LSTN and YSZ = CGO was used for the phase assignment.
- Ni-CGO-like system: $\min\left(\sigma_{\mathrm{rel,eon,comp}}, \sigma_{\mathrm{rel,CGO}}\right)$, where $\sigma_{\mathrm{rel,eon,comp}}$ is the relative el. composite conductivity and $\sigma_{\mathrm{rel,CGO}}$ is the single-phase relative ionic conductivity of the CGO-phase. Ni = LSTN and CGO = CGO was used for the phase assignment. (For simplicity, the same ratio of intrinsic conductivities was used as for LSTN/CGO)
- LSTN-CGO- system: $\min\left(\sigma_{\mathrm{rel,eon,comp}}, \sigma_{\mathrm{rel,ion,comp}}\right)$, where $\sigma_{\mathrm{rel,eon,comp}}$ and $\sigma_{\mathrm{rel,ion,comp}}$ are the relative electronic and the relative ionic composite conductivities.

The colours of the design regions are defined as follows.

- Red: The relative ionic or electronic conductivity drops below 0.01, which is interpreted to be a critical value for harmful loss of percolation. Note that this red stage is only reached for domains limited by single phase conductivities.

- Orange: The relative ionic and electronic conductivity are between 0.01 to 0.05, which are relatively low values but with a certain tolerance to complete failure.
- Yellow: The relative conductivities are in an intermediate range of 0.05 to 0.1.
- Green: The relative ionic and electronic conductivities are both above 0.1.

It is clearly visible that the Ni-YSZ system has the smallest design space (largest red space, respectively), because both phases need to provide a sufficient single-phase conductivity without percolation loss. For the Ni-CGO system, this restriction only applies for the CGO-phase, which is the only phase with ionic conductivity. For the electronic conductivity, both phases contribute and therewith the percolation-loss of the Ni-phase is uncritical. For the titanate CGO-system, the entire space used for the study belongs to the design space (no red zones). Moreover, also the green zone is significantly larger compared to the other material systems. It has to be emphasized, that this larger design-space does not only opens new possibilities for the design of well performing electrodes. Beyond that aspect, it also documents a certain tolerance (and associated robustness) for eventual deviations from the optimal design-points, which may originate from variations in the manufacturing process and/or from microstructure degradation.
Note that using this contour plot as a criterion for microstructure design may be too simple. E.g. for the Ni-YSZ system, where the electronic conductivity of Ni is orders of magnitudes larger than the ionic conductivity of YSZ, the optimal composition certainly shifts more towards larger YSZ contents than what is suggested from the contour plot. However, the Ni-phase also needs a sufficient margin to percolation loss e.g. due to degradation effects like Ni-coarsening, which can be captured more easily with the relative conductivity.

References

[1] M. S. Khan, S. B. Lee, R. H. Song, J. W. Lee, T. H. Lim, and S. J. Park, “Fundamental mechanisms involved in the degradation of nickel–yttria stabilized zirconia (Ni–YSZ) anode during solid oxide fuel cells operation: A review,” Ceram. Int., vol. 42, no. 1, pp. 35–48, 2016, doi: 10.1016/j.ceramint.2015.09.006.

[2] D. Burnat, G. Nasdaurk, L. Holzer, M. Kopecki, and A. Heel, “Lanthanum doped strontium titanate - ceria anodes: deconvolution of impedance spectra and relationship with composition and microstructure,” J. Power Sources, vol. 385, no. February, pp. 62–75, 2018, doi: 10.1016/j.jpowsour.2018.03.024.

[3] P. Marmet et al., “Generation of virtual three-phase Structures based on Gaussian Random Fields: An important Option for Digital Materials Design of Solid Oxide Fuel Cell Electrodes,” in GeoDict User Meeting 2021, 2021, p. 22.

[4] H. Moussaoui et al., “Stochastic geometrical modeling of solid oxide cells electrodes validated on 3D reconstructions,” Comput. Mater. Sci., vol. 143, pp. 262–276, 2018, doi: 10.1016/j.commatsci.2017.11.015.

[5] P. Marmet et al., “Modeling the impedance response and steady state behaviour of porous CGO-based MIEC anodes,” Phys. Chem. Chem. Phys., vol. 23, no. 40, pp. 23042–23074, 2021, doi: 10.1039/d1cp01962g.

[6] X. Zhou, N. Yan, K. T. Chuang, and J. Luo, “Progress in La-doped SrTiO3 (LST)-based anode materials for solid oxide fuel cells,” RSC Adv., vol. 4, no. 1, pp. 118–131, 2014, doi: 10.1039/c3ra42666a.

[7] O. Stenzel, O. Pecho, L. Holzer, M. Neumann, and V. Schmidt, “Predicting effective conductivities based on geometric microstructure characteristics,” AIChE J., vol. 62, no. 5, pp. 1834–1843, 2016, doi: 10.1002/aic.15160.

Keywords: EFCF 2022, Solid Oxide Technologies, SOC, Fuel Cells, SOFC, Titanate, CGO, Digital Microstructure Design, stochastic microstructure digital twin